



## An Alternative Numerical Model for Investigating Three-Dimensional Steam Turbine Exhaust Hood

S. Sadasivan<sup>1</sup>, S. K. Arumugam<sup>2†</sup> and M. C. Aggarwal<sup>3</sup>

<sup>1</sup>*School of Mechanical Engineering, Vellore Institute of Technology, India*

<sup>2</sup>*CO<sub>2</sub> Research and Green Technologies Centre, Vellore Institute of Technology, India*

<sup>3</sup>*Department of Mechanical Engineering, Gannon University, PA, USA*

†*Corresponding Author Email: asenthilkumar@vit.ac.in*

(Received April 8, 2019; accepted August 3, 2019)

### ABSTRACT

A proper design of exhaust hood geometry is very much essential in order to improve the overall efficiency of the steam turbine plant. The geometry of the non-axisymmetric exhaust hood makes the fluid flow at the exit of the steam turbine to be radially and circumferentially non-uniform. This work involves computational simulation of steam turbine asymmetric exhaust hood flows by incorporating the actuator-disc concept. The ANSYS FLUENT, finite volume based CFD solver is used for the present computational study. In the present simulation, the implementation of actuator disc boundary conditions with and without tip leakage is described in detail. The Actuator disc model approach exhibits a similar steam turbine exhaust hood flow asymmetry and static pressure recovery compared with the results reported in the literature, highlighting the applicability of the present model in coupling the rotor tip leakage jet with the steam turbine hood flow structure with less computational effort.

**Keywords:** Steam turbine; Exhaust hood; Actuator disc Model; CFD.

### NOMENCLATURE

ADM	Actuator Disc Model	$\tilde{u}_i$	velocity components
$C_p$	static pressure recovery coefficient	$x_i$	Cartesian space components
LSB	Last Stage Blade		
$K$	molecular heat conductivity		
$t$	time	$\tilde{h}$	enthalpy
$P_T$	total pressure	$\tilde{h}_i$	total enthalpy of the main flow
$\tilde{T}$	temperature	$k$	turbulent kinetic energy
$\tilde{p}$	pressure	$\mathcal{E}$	dissipation rate
$\tilde{\rho}$	density	$\mu$	molecular dynamic viscosity
$\gamma$	specific heat ratio	$\mu_T$	eddy viscosity

### 1. INTRODUCTION

Steam turbine is the predominant thermal energy conversion device used throughout the world for the production of electricity. The continuing increase in the cost of fuel combined with the decrease in the availability of energy sources highlights the importance of increasing the efficiency of the existing steam power plants. The steam turbine exhaust hood is a vital research area in the field of turbomachinery as its performance significantly influences the turbine power output.

An exhaust hood converts the kinetic energy of the leaving steam from the turbine into pressure energy, a process called static pressure recovery. The power output of the turbine is more when the exit pressure of the turbine is lower than that of condenser pressure. A properly designed exhaust hood can help in diffusing the flow from turbine exit pressure to condenser pressure. Design optimization of an exhaust hood necessitates a thorough understanding of fluid flow behavior in the exhaust hood (Wang *et al.*, 2010). The steam turbine exhaust hood consists of an axial-radial

diffuser and a collector, and has a complex geometry connecting the circular annulus turbine exit section to the condenser inlet which is placed perpendicular to the turbine axis rotation and making the flow direction change by  $90^\circ$  in a very short distance. This makes the flow through an exhaust hood asymmetric and vortical (Beevers *et al.*, 2010).

Exhaust hood design has been a topic of vibrant research for the last two decades. A full sized or scaled experimental testing is very expensive and hence CFD provides new opportunities in exhaust hood performance investigations. The non axis-symmetric geometry of exhaust hood and the interaction between the turbine and the hood are creating a highly non uniform flow at the inlet plane of the hood. This in turn creates a significant challenge in specifying the boundary conditions at the inlet plane of the exhaust hood during the computational study. Therefore it is clear that the most accurate results are obtained in CFD analysis when the turbine is coupled to the exhaust hood. However, modeling the full three dimensional geometry with unsteady, wet steam,  $360^\circ$  rotational flow path of the turbine stage, coupled to the exhaust hood creates challenges for even modern computing power. This necessitates the use of low-fidelity numerical models to reduce the computational demand to levels suitable for use in industrial design processes over the last two decades. A summary of these methods which couple the turbine last stage and the exhaust hood has been discussed by Burton *et al.* (2013). The simulation of isolated exhaust hood from the last stage blade could drastically reduce the computational power. However, the result obtained from the isolated model highly depends on the inlet flow conditions (Tindell *et al.*, 1996). In isolated models, the flow conditions are to be obtained experimentally from the outlet of the last stage blade of the rotor for generating the representative flow fields.

The first comprehensive model is proposed by Benim *et al.* (1995), for capturing the interaction between the LSBs and the exhaust hood through an iterative technique. The flow interaction between the exhaust hood and the LSBs and their 3-D effects on turbine stage efficiencies are carefully carried out numerically by Tanuma *et al.* (2014, 2013). Finzel *et al.* (2013) presented detailed research on the static pressure recovery of low pressure steam turbine exhaust hoods including the influence of outflows from the last stage of turbine. All the research work have shown that adding the last stage blades into the steam turbine exhaust hood study is highly unavoidable. The mixing-plane method (Fan *et al.*, 2007) is one of the efficient methods in CFD for capturing the flow interactions by circumferentially averaging the flow behavior in the mixing plane. However, this approach fails to generate the non-uniform flow pattern at the exhaust hood inlet due to the asymmetric geometry of the exhaust hood. Fu *et al.* (2007) suggested an alternative technique called the frozen rotor method for capturing the

asymmetric inlet flow by modeling all the blade passages. However, it is more computationally demanding with extra cell count about 50 million and cannot be used for the design development. Stein *et al.* (2015) have proposed a novel multiple mixing plane approach for coupling the last stage blades and the exhaust hood. They have successfully proved that this method is more accurate than the frozen rotor method and comparatively less computationally demanding at the same time. These above discussed methods are generally computationally demanding and hence not suitable for design calculations where multiple iterations are required. Rather they can be used as validation tools. This necessitates the development of further low-fidelity numerical models.

The ADM approach is one of the low-fidelity numerical models, which has comparable solution accuracy and reduced computational cost. The ADM is used to study the flow pattern across the wind turbines. Relative studies between ADM and 3-D rotor CFD models (Rethore *et al.*, 2008) show that the ADM approach is sufficient to capture the time-averaged effect of the real turbine rotor, with a significantly lowered computational effort, almost of two orders of magnitude lesser than that of a full scaled model of the rotor. Liu and Hynes (2002, 2003) have developed a multi-block 3D solver, incorporating an ADM to calculate the asymmetric nature of flows in the coupled domain of LSBs and the exhaust hood. However, this approach has not been widely accepted due to the negligence into considerations of the rotor tip leakage and choking effects: both of which remarkably effects on the exhaust hood flow structure. Tadj *et al.* (2001) emphasized the importance of considering tip leakage jet effects on the exhaust hood flow structure. They concluded that both tangential steam blowing and the steam leaking through the rotor blade of the turbine last stage contributes to enhancing the stabilization of the boundary layer of the exhaust hood. Hence, by considering above discussed important factors, this research work intends to perform CFD modeling of an exhaust hood using the actuator disk method including the tip leakage effects.

The present research aims an extension of the ADM to represent the LSB rows with and without tip clearness in highly flared annuli. The ADM approach and the execution of disc boundary conditions are described in detail. The developed method is validated by comparing with the reported results in the literature. The obtained results are analyzed in terms of static pressure recovery, flow structure, and computational efforts.

## 2. COMPUTATIONAL MODEL

The present calculations employ the ADM approach for studying the flow behavior in a steam turbine exhaust hood. The numerical studies are carried out with and without tip leakage jets to investigate the mutual interaction of the exhaust hood and the LSBs. The finite volume based CFD solver ANSYS FLUENT is used in the current research solves

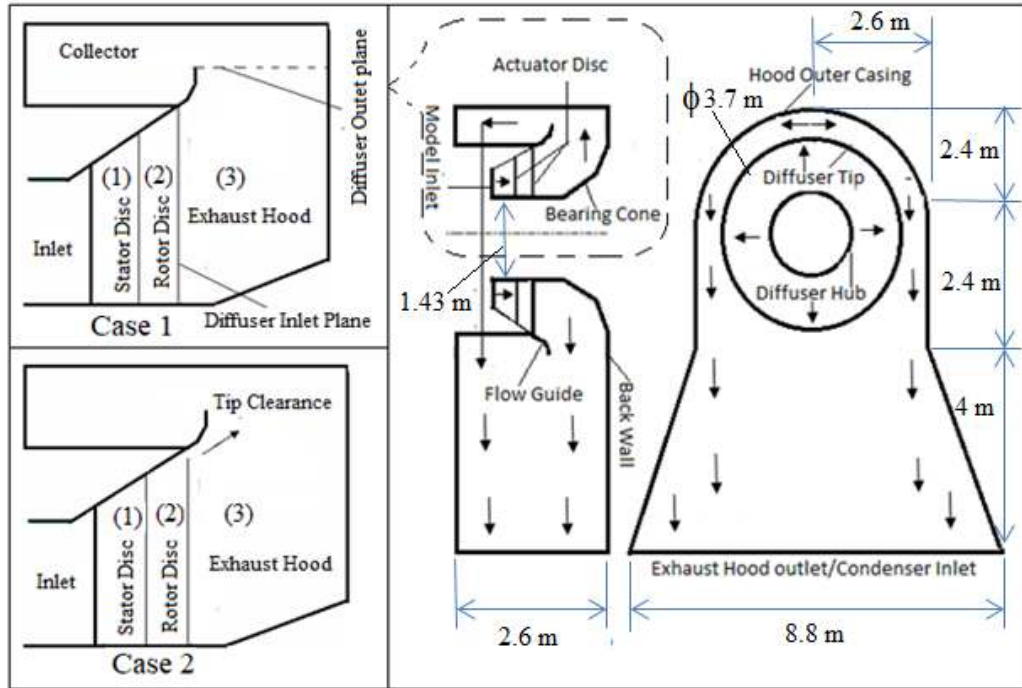


Fig. 1. Schematic representation of turbine-diffuser model.

the compressible flow governing continuity, momentum, and energy equations. These flow governing equations along with the equations of  $k-\varepsilon$  turbulence model can be written in tensor form as,

$$\frac{\partial}{\partial x_j} (\bar{\rho} \tilde{u}_j) = 0 \quad (1)$$

$$\frac{\partial}{\partial x_j} (\bar{\rho} \tilde{u}_i \tilde{u}_j) = -\frac{\partial \bar{p}}{\partial x_j} \delta_{ij} + \frac{\partial (\bar{\tau}_{ij} - \bar{\rho} \tilde{u}_i'' \tilde{u}_j'')}{\partial x_j} \quad (2)$$

$$\frac{\partial}{\partial x_j} [\bar{\rho} \tilde{u}_j \tilde{h}_t] = \frac{\partial [\tilde{u}_i (\bar{\tau}_{ij} - \bar{\rho} \tilde{u}_i'' \tilde{u}_j'') - (\bar{q}_j + \bar{\rho} \tilde{e}'' \tilde{u}_j'')] }{\partial x_j} \quad (3)$$

$$-P_k + \bar{\rho} \tilde{\varepsilon}^* + 2\mu \frac{\partial \sqrt{k}}{\partial x_j} \frac{\partial \sqrt{k}}{\partial x_j}$$

The transport equation of kinetic energy

$$\frac{\partial}{\partial x_j} (\bar{\rho} \tilde{u}_j k) = \frac{\partial}{\partial x_j} \left[ \left( \mu + \frac{\mu_T}{\sigma_k} \right) \frac{\partial k}{\partial x_j} \right] + P_k - \bar{\rho} \tilde{\varepsilon}^* - 2\mu \frac{\partial \sqrt{k}}{\partial x_j} \frac{\partial \sqrt{k}}{\partial x_j} \quad (4)$$

The transport equation of dissipation rate

$$\frac{\partial}{\partial x_j} (\bar{\rho} \tilde{u}_j \varepsilon^*) = \frac{\partial}{\partial x_j} \left[ \left( \mu + \frac{\mu_T}{\sigma_\varepsilon} \right) \frac{\partial \varepsilon^*}{\partial x_j} \right] + C_{\varepsilon 1} P_k \frac{\varepsilon^*}{k} - C_{\varepsilon 2} f_{\varepsilon 2} \bar{\rho} \frac{\varepsilon^{*2}}{k} + 2 \frac{\mu \mu_T}{\bar{\rho}} \left( \frac{\partial^2 \tilde{u}_i}{\partial x_j \partial x_j} \right) \left( \frac{\partial^2 \tilde{u}_i}{\partial x_l \partial x_l} \right) \quad (5)$$

$$\bar{p} = \bar{\rho} R \tilde{T} = \bar{\rho} \frac{\gamma - 1}{\gamma} h = \bar{\rho} (\gamma - 1) \tilde{e} \quad (6)$$

where,

$$-\bar{\rho} \tilde{u}_i'' \tilde{u}_j'' = \mu_T \left[ \frac{\partial \tilde{u}_i}{\partial x_j} + \frac{\partial \tilde{u}_j}{\partial x_i} \right] - \frac{2}{3} \mu_T \frac{\partial \tilde{u}_j}{\partial x_j} \delta_{ij} - \frac{2}{3} \bar{\rho} k \delta_{ij}$$

$$\bar{\tau}_{ij} \cong \mu(\tilde{T}) \left[ \frac{\partial \tilde{u}_i}{\partial x_j} + \frac{\partial \tilde{u}_j}{\partial x_i} \right] - \frac{2}{3} \mu \frac{\partial \tilde{u}_j}{\partial x_j} \delta_{ij}$$

$$\bar{\rho} \tilde{e}'' \tilde{u}_j'' = -K_T \frac{\partial \tilde{T}}{\partial x_i}$$

$$P_k = -\frac{1}{2} \bar{\rho} \tilde{u}_i'' \tilde{u}_j'' \left[ \frac{\partial \tilde{u}_i}{\partial x_j} + \frac{\partial \tilde{u}_j}{\partial x_i} \right]$$

$$\bar{q}_i \cong -k(\tilde{T}) \frac{\partial \tilde{T}}{\partial x_i}$$

The molecular diffusion coefficient and the turbulent model constants are

$$f_{\varepsilon 2}(\text{Re}_T) = 1 - 0.3e^{-\text{Re}_T^2}; \quad \text{Re}_T = k^2 / \nu \varepsilon^*$$

$$C_{\varepsilon 1} = 1.44; \quad C_{\varepsilon 2} = 1.92; \quad \sigma_k = 1; \quad \sigma_\varepsilon = 1.3$$

## 2.1 Geometry and Meshing Details

The test geometry for the present flow simulation is the modified geometry of Durham last stage turbine and exhaust hood developed by [Burton \*et al.\* \(2014\)](#) free from commercial restriction, which has been proved to generate a representative flow structure. A schematic representation of the computational domain which includes the last stage turbine row and the entire exhaust hood is shown in Fig. 1(a). The meshes are developed separately using ICEM CFD for different parts, namely

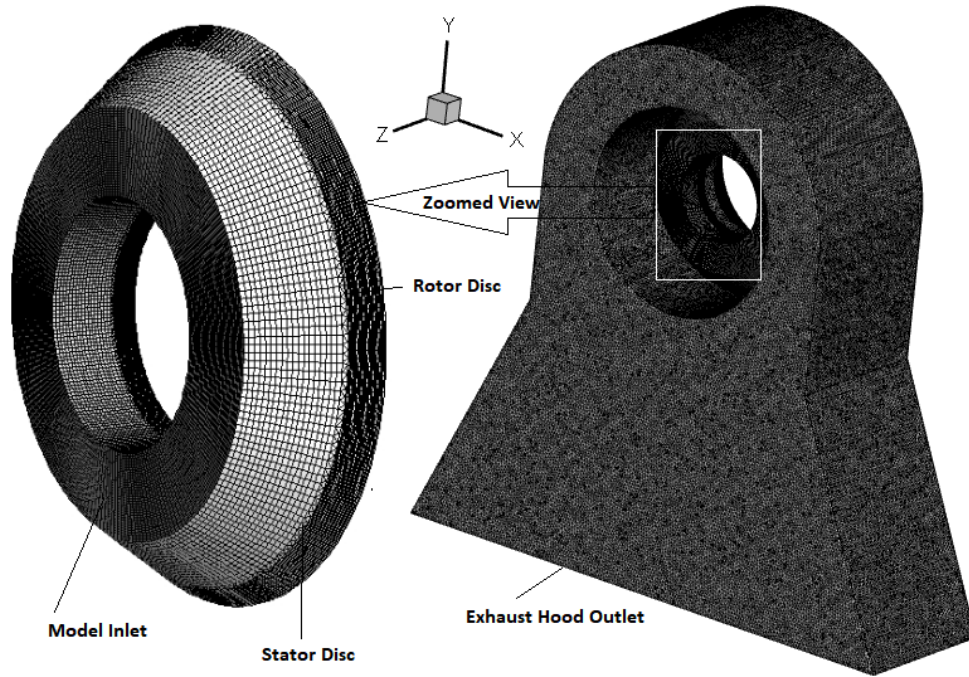


Fig. 2. Computational domain marked with boundary conditions.

- (1) Inlet-stator section
- (2) Stator-rotor section
- (3) Rotor –Exhaust hood Section

In the present study, the rotor and stator that form the last stage of the turbine are modeled as two infinitely thin discs. The underlined assumption of the ADM method is that the flow effects induced by an actual three-dimensional turbine stage can be replicated by incorporating suitable jump conditions across these two thin discs. The meshing of the present computational domain mainly consists of two steps. Firstly, the actuator discs of negligible thickness are to be provided with a surface mesh. The domain construction must ensure two different faces of the actuator disc, although it is a two-dimensional lamina. The volume meshing has to be performed for the actuator disc part of the computational domain to represent the flow domain corresponding to the last stage of the turbine. Secondly, the construction of the computational domain includes three-dimensional modeling and meshing of the exhaust hood part. In the present study, a structured block was generated for the first part of the computational domain with 0.4 million cells whereas two unstructured blocks were created for part two and three due to their complexity. The meshes for all the parts were generated with a variation of  $y^+$  between 30 and 200. Also, all the computational domain meshes satisfy the requirement of quality in terms of skewness greater than 10 and the expansion ratio less than 3. A grid independence investigation has been conducted to eliminate the grid resulting error percentage in the solution. Three-dimensional mesh used for the current study is shown in Fig. 2. The different plane locations used in the result analysis of the current

simulations are also shown in Fig. 2(b).

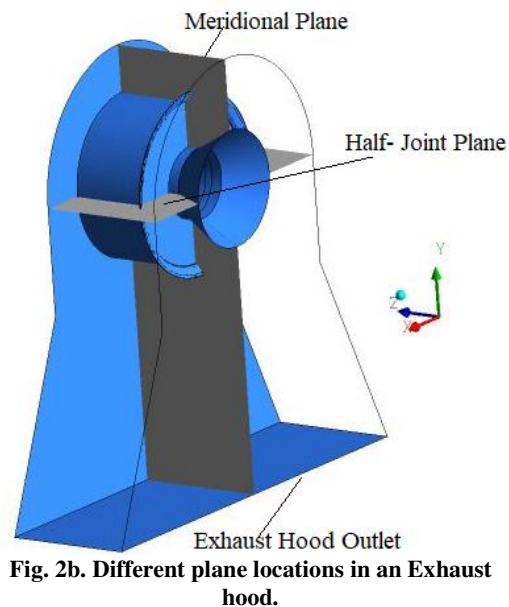
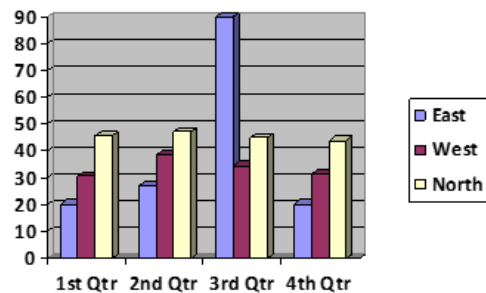


Fig. 2b. Different plane locations in an Exhaust hood.

### 3. DETAILS OF ACTUATOR DISC MODEL

In the present simulations, the last stage blades were contracted into zero thickness permeable discs at the trailing edge of the turbine blade rows. The behavior of steam flow across the discs can take a discontinuous jump to capture the steam flow turning and entropy generation in the LSB rows. Liu and Hynes (2002, 2003) have presented the behavior of the ADM in the computational domain as shown in Fig. 3. The upstream side of the disc represents the inlet of the turbine blade row and the downstream side the outlet of the blade row. The specified numerical boundary has been generated by the mesh interface treatment in the three domains. The energy transfer happening in the real turbine stage is represented here by specifying the pressure drop across the actuator disc as a function of flow velocity and those values are calculated from the turbine blade specifications reported in Burton *et al.* (2015). The representative profile of velocity distribution was applied at the disc boundary as represented in Fig. 4.

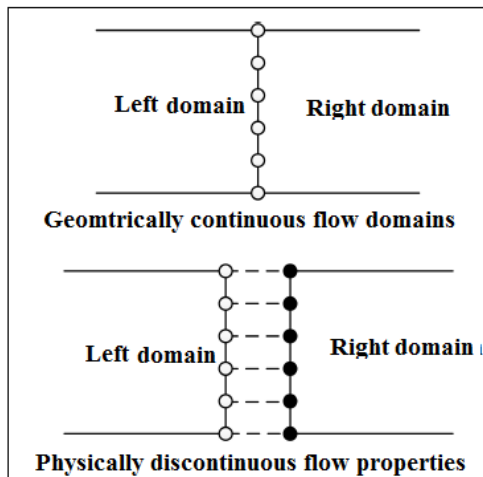


Fig. 3. Schematic representation of the ADM by Liu and Hynes (2002, 2003).

The following assumptions are made for the implementation of the ADM approach in the current simulations.

- In the meridional plane, the mass flow is conserved.
- The entropy variations depend on the blade loss coefficients applied at the blade row.
- Infinitely thin discs cannot provide any kind of opposition to steam flowing through it.

#### 3.1 Numerical Boundary Conditions

In the present computational domain, the different boundary conditions used are 'Pressure Inlet', 'Pressure Outlet', 'Wall' and 'Fan'. The total pressure and total temperature values were specified at the inlet of the computational domain are 26800 Pa and 339.5 K, respectively. The exhaust hood outlet static pressure was set at 10000 Pa. In the

solid wall, the flow is assumed to be adiabatic. The static pressure drop across the actuator discs is calculated from the turbine stage specifications reported by Burton *et al.* (2012) is shown in Table 1. The specifications details for 'Fan' boundary are shown in Table 2. The working fluid used for the current calculation is water vapor, modeled as perfect gas with the properties of  $C_p = 4153 \text{ J/kgK}$ ,  $\gamma = 1.12$ , Thermal Conductivity =  $0.061 \text{ W/mK}$ , and the Dynamic Viscosity of  $1.032 \times 10^{-5} \text{ Pas}$ .

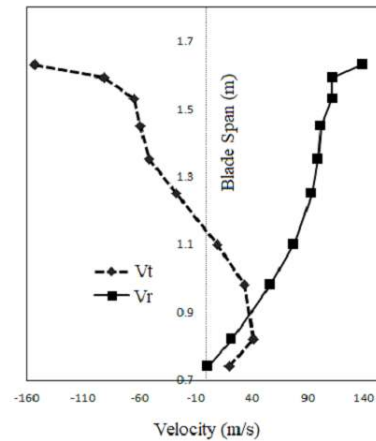


Fig. 4. Velocity profile applied at the actuator disc plane.

Table 1 Parameters employed in the current simulation

Specification of parameters for Turbine Stage	
Hub/Tip ratio	0.44
Turbine outlet static pressure	8800 Pa
Mass flow rate	86.6 m/s
Rotor Speed	3000 rpm
Total Temperature	339.5 K
Pressure ratio	0.292

Table 2 Boundary conditions

Boundary conditions for Actuator discs	
Numerical Boundary Type	Fan
Static Pressure drop (Pa)	Constant for Stator : 12889.74 for Rotor : 4901.50
Pressure Jump Specification	Calculate pressure drop from average conditions

## 4. RESULT AND DISCUSSION

### 4.1 ADM Approach without Tip Leakage Flows

The main focus of any CFD study of an exhaust hood is the accurate capturing of the flow structure and its interaction effects. One unique feature of the

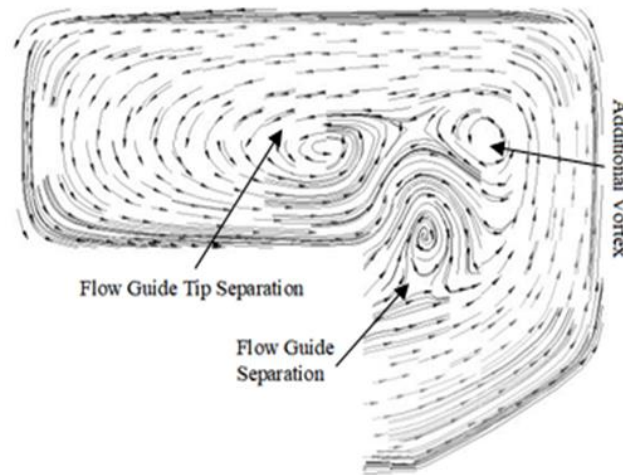


Fig. 5. Stream traces within the meridional plane of the diffuser.

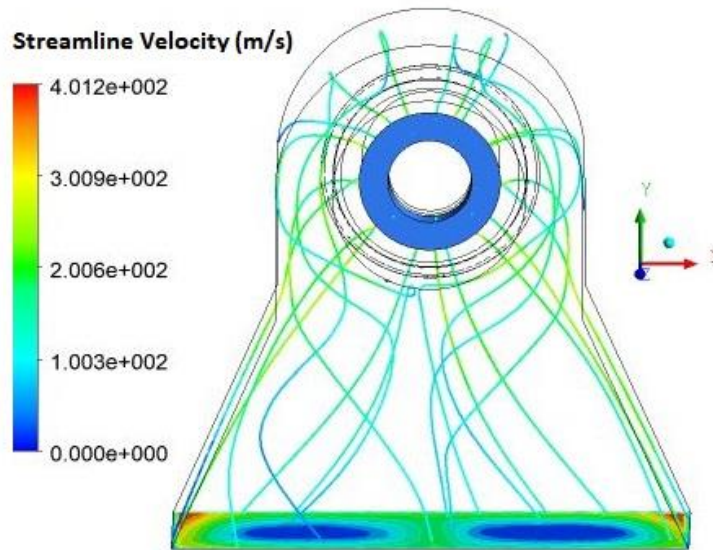


Fig. 6. Stream traces from the inlet to outlet of the exhaust hood computational domain.

exhaust hood's flow structure is its asymmetric nature, due to the non-axisymmetric geometry of the exhaust hood. A comparison of present results with the numerical results of [Burton \*et al.\* \(2012-2015\)](#), shows that the present simulations with the ADM have successfully captured all the flow separations within the hood as shown in Fig. 5. Initially, large vortices are generating around the tip region and progress downstream along the direction of flow to form a couple of counter-rotating vortices in the condenser neck, as shown in Fig. 6. The velocity vector at the exhaust hood outlet plane in Fig. 6 shows a reverse flow pattern at the core of each vortex. The low energy vortex at the center of the exhaust hood outlet drives the main quantity of flow outward to the condenser neck wall. This results in a higher magnitude in velocities at the exhaust hood back wall and bulk quantity of non-uniform flow discharging down to the end walls. The vortices inside the diffuser and the collector are the main source of high pressure loss in the steam

turbine exhaust hood. In order to understand the complexity of flow pattern in the exhaust hood, velocity vector plots have been made at the various locations of the exhaust domain as shown in Figs. 8 and 9. It can be noticed that the ADM is capable of capturing all the flow interactions within the exhaust hood, thus validated the suitability of the present computational framework for coupled turbine-exhaust hood simulation. It is also observed that the present ADM has the potential to reduce computational effort, as it eliminates the computation of flow field in the turbine blade rows. Moreover, the current approach does not necessitate mesh reconstruction, thus help in saving the computational time required for the re-computing of node and face data.

#### 4.2 ADM Approach with Tip Leakage Flows

During the first phase of the current research, the ADM has successfully captured all the flow behavior in the exhaust hood. However, the

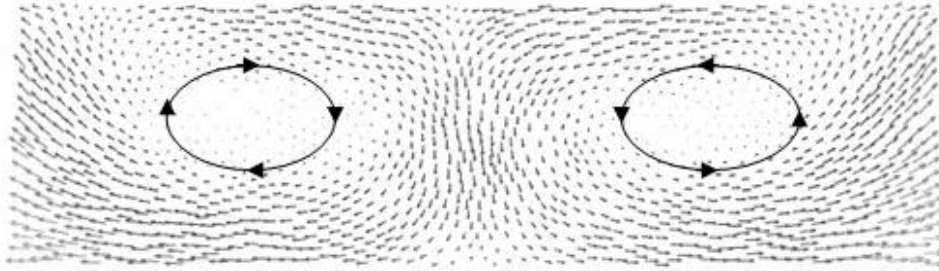


Fig. 7. Velocity vector in the exhaust hood outlet plane.

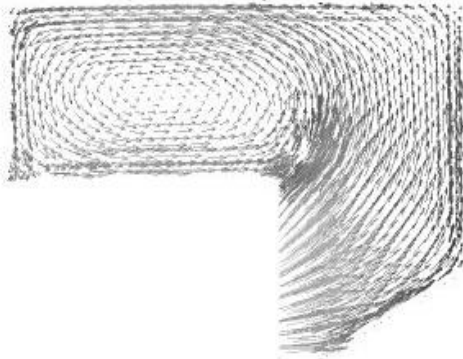


Fig. 8. Velocity vector in the meridional plane.

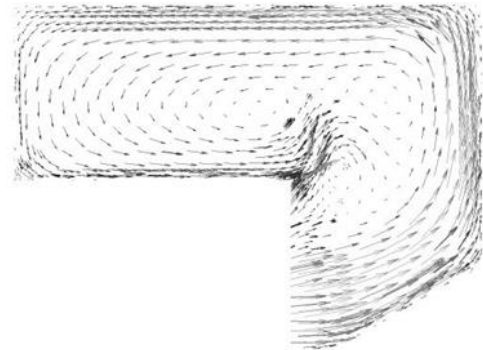


Fig. 9. Velocity vector in the half joint plane.

literature review has highlighted the importance of including the rotor tip leakage jet effects on the exhaust hood performance. Therefore, upon verifying the validity of the ADM, the aim of the current research got shifted to the exploration of the effects of rotor tip leakage on exhaust hood flow behavior. During the second phase, the geometry was modified to include the rotor tip gap of 0.5% of the blade height. The Stator-Rotor section and Rotor-Exhaust hood section were re-meshed using ICEM CFD meshing software to include the rotor tip gap. The meshes for the parts were generated with a variation of  $y^+$  between 30 and 200 for meeting the  $y^+$  requirement of the  $k - \epsilon$  model with the standard wall functions. The computational domain for phase two was modelled by following the same strategy as in phase one and also the solution set up was retained the same. The steady-state results obtained from the simulations are then used here to explore the effect of tip leakage jet on the flow pattern within the steam turbine exhaust hood.

The pressure distribution along the radial direction at the exit of the rotor from the ADM with rotor tip leakage jet is compared with the experimental result of Gardzilewicz *et al.* (2003), shown in Fig. 10. The magnitude of total pressure distribution in the normalized blade span cannot be directly compared due to the different operating conditions. However, the shape of the profile is in a good agreement with the reported work, with an approximately uniform pressure profile between 0.0 and 0.8 normalized blade span. In the comparative study, significant

deviations are found in the rotor tip region. This is due to the tip leakage jet effects on the exhaust hood flow structure. The closely matching results in Fig.10 prove the capability of the present ADM approach in capturing the overall flowfield behind the turbine blades with tip leakages.

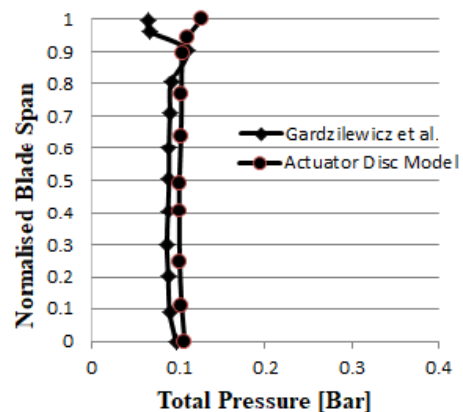
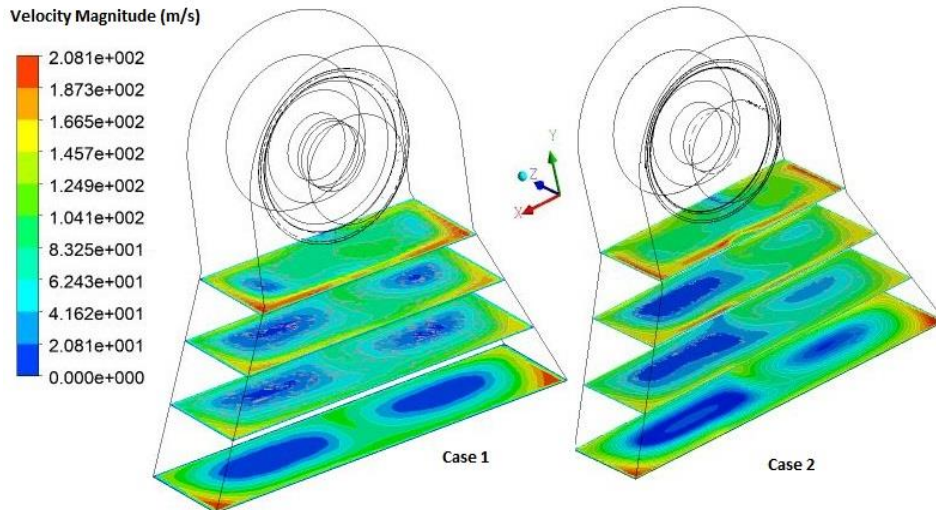


Fig. 10. Comparison of total pressure distribution at the rotor outlet.

#### 4.3 Comparative Study between ADM Approach with and without Rotor Tip Leakage Jet

A comparison of velocity variation obtained with and without tip leakage jet at four different sections in the direction of flow moving to the exhaust hood outlet is shown in Fig. 11. In both cases, the swirl begins to separate at the diffuser section and



**Fig. 11. Velocity contours of four level sections at exhaust hood outlet Case 1) Without rotor tip leakage, Case 2) With rotor tip leakage.**

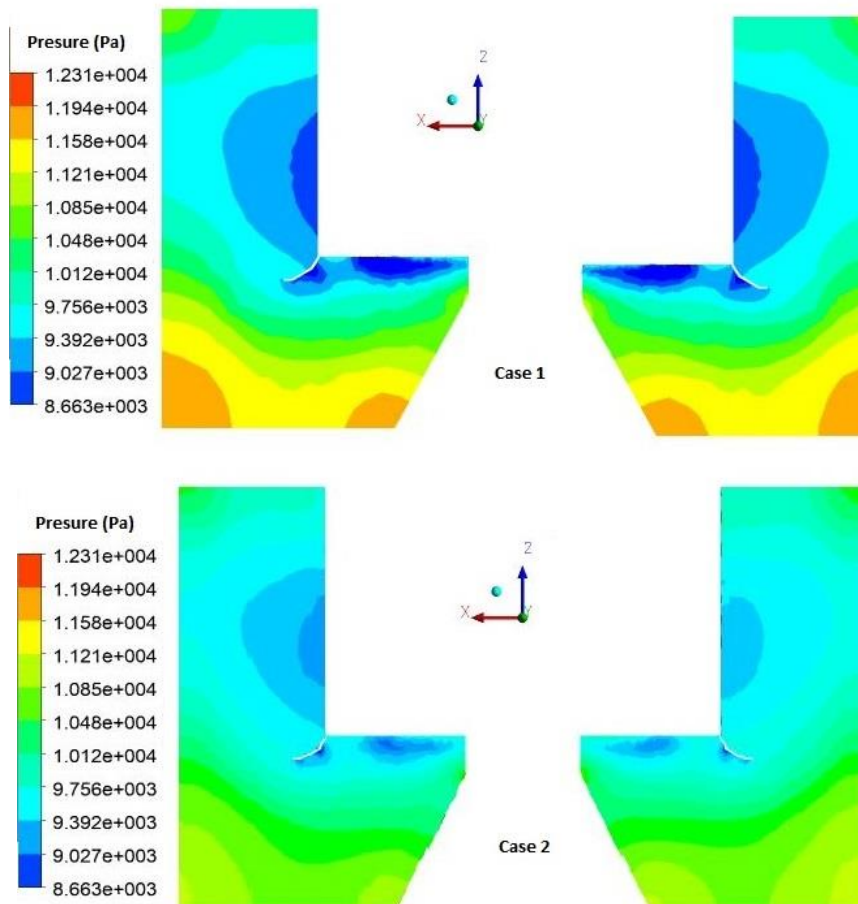


**Fig. 12. Pressure contour at half joint plane Case 1) Without rotor tip leakage, Case 2) With rotor tip leakage.**

continues to grow till the outlet of the exhaust hood. When case 2 is compared with case 1, the downflow is more asymmetric in nature with the addition of tip clearance as shown in Fig. 11. This is

because of the high momentum jet energize the fluid flow along the direction of the flow guide, decreasing the magnitude of the low pressure region within the exhaust hood. In addition, the amount of



the low pressure region behind the exhaust hood flow guide has also decreased due to the reduced strength of the vortex developed in the upper part of the steam turbine exhaust hood is shown in Fig. 12. Reduced vortex strength reduces the blockage effects in the collector and adds to the higher pressure recovery throughout the exhaust hood.

However, the magnitude of reduction in the low pressure region on the left and right-hand side of the exhaust hood is not uniform. This non-uniformity is due to the change in tangential velocity of flow entering into the exhaust hood inlet by the addition of tip leakage. The high momentum jet from the tip clearance of the last stage blade adds more fluid flow at the outer radius, increasing the tip swirl and driving more quantity of fluid on the left-hand side of the steam turbine exhaust hood. Although the increased asymmetric nature of the flow is contributing a negative impact on the characteristics of the exhaust hood flows, the positive impact of the tip leakage flows around the flow guide region is more significant than the flow asymmetry disadvantages. The present results highlight the importance of considering tip leakage modeling to develop an exhaust hood flow structure with reasonable accuracy.

### 4.3.1 Total Pressure

The total pressure profile is one of the significant flow aspects influencing the vortices formation within the exhaust hood, [Fu et al. \(2007\)](#). The total pressure profile at the outlet of the rotor blades obtained by the ADM is compared with that obtained by other simplified models in Fig. 13. The total pressure distribution profiles are obtained with current ADM approach are consistent with that derived using other reported methods on the same geometry. It can be observed that the result obtained from the present ADM model including the tip leakage jets is in good agreement with that of the frozen rotor method and the isolated model including the leakage effects in the boundary conditions. Further, the result obtained using the ADM without including the tip leakage is also in close agreement with that obtained from the isolated model without including the jet effects. Moreover, it can be noticed that the values of total pressure at the tip of the blade are about 0.13 bar for the models that included the leakage effects, whereas the values of total pressure are around 0.11 bar for the models without including the effects of tip jets. This emphasizes the importance of including the tip leakage jets in the models.

### 4.3.2 Static Pressure Recovery

Static pressure recovery coefficient,  $C_p$  is one of the most important factors for evaluating the performance of the exhaust hood. It is expressed in Eq. (5), where  $P_m$  and  $P_{t_{in}}$  are the averaged static pressure and the total pressure at the inlet of the steam turbine exhaust hood and  $P_{out}$  is the average static pressure in the exhaust hood outlet. The values of static pressure coefficients calculated with different numerical modeling of the exhaust hood

are compared in Table 3. Under ideal conditions, the static pressure recovery coefficient value is one at which all of the kinetic energy of the exhaust flow from the turbine blades would be converted into pressure energy when the flow is passing through the diffuser and all the losses associated with the exhaust hood is zero. This results in a minimum value of static pressure at the exit of the turbine stage, hence a maximum turbine power output. In a real case, only some part of the kinetic energy is recovered in the diffuser section and there will be some pressure losses associated with the exhaust hood due to friction and flow separations. A positive value of the pressure recovery coefficient will create a higher power output as the pressure at the outlet of the steam turbine is lower and thus there is a greater enthalpy drop across the steam turbine. Static pressure recovery coefficient value for a real exhaust hood is less than one and often negative value.

$$C_p = \frac{P_{out} - P_{in}}{P_{t_{in}} - P_{in}} \quad (7)$$

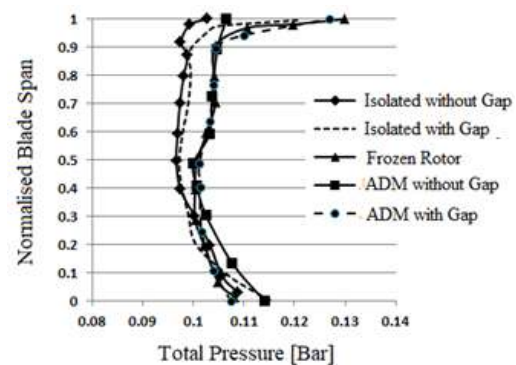


Fig. 13. Total pressure variations at the rotor outlet.

The calculated values of static pressure recovery coefficient from different approaches are tabulated in Table 3. The variations in the  $C_p$  is likely due to the interaction between coupled domains, as the boundary condition downstream of the last stage turbine blade will be influenced by the flowfield in the hood, [Veerabathraswamy et al., 2016](#)). The values of  $C_p$  from the CFD analysis of an isolated exhaust hood without tip leakage ([Burton et al., 2012](#)) is -0.035 and from the present ADM without tip leakage is 0.202. The pressure recovery capacity of the exhaust hood is more accurate in the present model due to the influence of flow interactions between the exhaust hood and the last stage blades. The coupling between the exhaust hood and the turbine stages has not been modeled in the isolated exhaust hood case but it is included in the ADM. This shows the importance of adding the last stage blades into the steam turbine exhaust hood study. It can also be observed that the  $C_p$  values obtained from the ADM and the isolated methods with considering the tip leakages jets are higher than those obtained from both methods without considering the tip leakage jets. The addition of tip

**Table 3 Comparison of Cp for different approaches**

No	Different Methods	Tip leakage	Cp	Total cell count (M)
1	Isolated Exhaust Hood	No	-0.035	2.0 (for LSB)+2.6 (for EH)=4.6
2	Isolated Exhaust Hood	Yes	0.236	2.2(for LSB)+ 2.6(for EH)=4.8
3	Frozen Rotor (Full annulus)	Yes	0.241	48.94
4	Actuator Disc Model (Present)	No	0.202	2.9
5	Actuator Disc Model (Present)	Yes	0.243	3.2

clearance increases the static pressure recovery coefficient of the exhaust hood in both the cases due to the high velocity of jet minimizing the low pressure region within the hood. The calculated Cp value for an isolated hood with tip leakage effects is 0.236 whereas when the frozen rotor approaches were applied to couple the steam turbine exhaust hood to the last stage, the calculated Cp value is 0.241. However, the isolated approach has not been suggested for the exhaust hood flow analysis due to the circumferential averaging of flow properties at the interface of the turbine stage and exhaust hood removes the flow asymmetry. In a real case, the exhaust hood flow structure is highly circumferentially and radial non-uniform due to the high degree of swirl angle from the rotation of the turbine blades and the non-asymmetric exhaust hood geometry. In the present simulations, these highly influential factors were considered and implemented on the same geometry by the ADM method. The calculated value of Cp for case 1 (ADM without tip leakage) is 0.202 and for case 2 (ADM with tip leakage) is found to be 0.243. The increment in the static pressure recovery coefficient of the exhaust hood is due to the impingement of high velocity jet on the flow along the flow guide. From the calculated results of Cp of the exhaust hood, it has shown that the ADM is very much suitable for capturing the effects of tip leakage as well as the effects of coupling the hood to the turbine LSBs.

The computational advantage of adopting the ADM method in the exhaust hood study can be well understood from Table 3. The present study employed just 3.2 million nodes for the entire domain and it is consumed a minimum computational time of 52 hours with 4 CPU and 8 GB of memory. The total numbers of nodes used for the frozen rotor approach with the full annulus and single passage are noted to be very high. The frozen rotor technique is a widely accepted numerical model for capturing asymmetric flow behavior in an exhaust hood. However, this method is computationally more demanding due to the large cell counts of about 50 million and the requirement of long computational times of 267 hours on 3 parallel computers and each with 4 CPU and 8 GB of memory. On the other hand, the actuator disc model cannot handle choking and associated effects. The last stage of the turbine blades is usually susceptible for choking. Methods like frozen rotor technique, multiple mixing plane model proposed by [Stein et al. \(2015\)](#) can very well handle choked flow conditions. This is the main limitation

of the present actuator disc model. Hence the ADM approach can be used as a design tool where multiple design iterations are required rather than as a validation tool. On the other hand, the actuator disc method would be very effective when the flow in the turbine rows is subsonic and unchoked. For the present simulations, the ADM approach is noted to be accurate enough in giving expected exhaust hood flow structure and for design development. The comparable predictions of ADM approach and the frozen rotor method with full annulus flow calculations support the use of ADM approach to have substantial saving in computational power, computational time.

## 5. CONCLUSION

The physics of flow behavior in the exhaust hood and the interaction among the collector, exhaust hood and the steam turbine have been investigated by incorporating the ADM with and without tip leakage. The implementation of the ADM in the numerical solution framework is presented in detail. The results obtained from the present study are consistent with other reported results, highlighting the applicability of ADM approach in coupling the rotor tip leakage and the steam turbine hood flow structure. Further, the present study revealed that the importance of including the tip leakage effects in the modeling to predict the exhaust hood performance accurately. The use of ADM approach is found to be computationally very cheaper. The savings in computational time is mainly due to the simplification of complex rotation of rotor blade as a thin disc with jump conditions applied. The total pressure recovery coefficient predicted using present the ADM approach is in good agreement with that of frozen rotor method. Hence this approach is recommended as an efficient and easily implementable technique for the preliminary design development of steam turbine exhaust hood. Moreover, the present study provides confidence for further investigations on other complexities of the exhaust hood flowfield using the ADM approach. One of the ongoing extension works is the analysis of multi-phase flow within the exhaust hood structure by considering unsteady wet steam modeling with internal furniture.

## REFERENCES

Beevers, A., F. Congiu, F. Pengue and T. Mokulys (2010, October). An analysis of the merits of

- CFD for the performance prediction of a low pressure steam turbine radial diffuser. In *ASME Turbo Expo 2010: Power for Land, Sea, and Air* (pp. 563-574). American Society of Mechanical Engineers
- Benim, A. C., M. Geiger, S. Doehler and M. Schoenenberger (1995). Modelling the flow in the exhaust hood of steam turbines under consideration of turbine-exhaust hood interaction. *VDI BERICHTE* 1185, 343-343.
- Burton, Z. (2014). *Analysis of low pressure steam turbine diffuser and exhaust hood systems* (Doctoral dissertation, Durham University).
- Burton, Z., Ingram, G. L., & Hogg, S. (2013). A literature review of low pressure steam turbine exhaust hood and diffuser studies. *Journal of Engineering for Gas Turbines and Power*, 135(6), 062001.
- Burton, Z., G. Ingram and S. Hogg (2015). Efficient Methods for Predicting Low Pressure Steam Turbine Exhaust Hood and Diffuser Flows at Design and Off-Design Conditions. *Journal of Engineering for Gas Turbines and Power* 137(8), 082601.
- Burton, Z., S. Hogg and G. Ingram (2012, June). A generic low pressure exhaust diffuser for steam turbine research. In *ASME Turbo Expo 2012: Turbine Technical Conference and Exposition* (pp. 455-466). American Society of Mechanical Engineers.
- Burton, Z., S. Hogg and G. L. Ingram (2014). The influence of inlet asymmetry on steam turbine exhaust hood flows. *Journal of engineering for gas turbines and power* 136(4), 042602.
- Fan, T., Y. Xie, D. Zhang and B. Sun (2007, January). A Combined Numerical Model and Optimization for Low Pressure Exhaust System in Steam Turbine. In *ASME 2007 Power Conference* (pp. 349-358). American Society of Mechanical Engineers.
- Finzel, C., M. Schatz, M. V. Casey and D. Gloss (2011, January). Experimental investigation of geometrical parameters on the pressure recovery of low pressure steam turbine exhaust hoods. In *ASME 2011 Turbo Expo: Turbine Technical Conference and Exposition* (pp. 2255-2263). American Society of Mechanical Engineers.
- Fu, J., J. Liu and S. Zhou (2007). Experimental and numerical investigation of interaction between turbine stage and exhaust hood. *Proceedings of the Institution of Mechanical Engineers, Part A: Journal of Power and Energy* 221(7), 991-999.
- Gardzilewicz, A. N. D. R. Z. E. J., J. Swirydzuk, J. Badur, M. I. C. H. A. Ł. Karcz, R. O. B. E. R. T. Werner and C. Z. E. S. Ł. A. W. Szyrejko (2003). Methodology of CFD computations applied for analysing flows through steam turbine exhaust hoods. *Transactions of the Institute of Fluid-flow Machinery* 113, 157-168.
- Liu, J. J. and T. P. Hynes (2002, January). The Investigation of Turbine and Exhaust Interactions in Asymmetric Flows: Part 2—Turbine-Diffuser-Collector Interactions. In *ASME Turbo Expo 2002: Power for Land, Sea, and Air* (pp. 179-188). American Society of Mechanical Engineers.
- Liu, J. J. and T. P. Hynes (2003). The investigation of turbine and exhaust interactions in asymmetric flows—blade-row models applied. *Journal of turbomachinery* 125(1), 121-127.
- Rethore, P. E. M., Sørensen, N. N., Zahle, F., & Johansen, J. (2008). Comparison of an actuator disc model with a full rotor cfd model under uniform and shear inflow condition. In *4th PhD seminar on wind energy in Europe*. European Academy of Wind Energy.
- Stein, P., C. Pfoster, M. Sell, P. Galpin and T. Hansen (2015, June). CFD Modeling of Low Pressure Steam Turbine Radial Diffuser Flow by Using a Novel Multiple Mixing Plane Based Coupling: Simulation and Validation. In *ASME Turbo Expo 2015: Turbine Technical Conference and Exposition* (pp. V008T26A020-V008T26A020). American Society of Mechanical Engineers.
- Tajc, L., L. Bednar, J. Polansky and E. I. Gudkov (2001). Exhaust Hoods of Double-Flow Arrangement. In *4th European Conference on Turbomachinery, Florence, Italy, March* (pp. 20-23).
- Tanuma, T., Y. Sasao, S. Yamamoto, Y. Niizeki, N. Shibukawa and H. Saeki (2014, June). Numerical Investigation of Steam Turbine Exhaust Diffuser Flows and Their Three Dimensional Interaction Effects on Last Stage Efficiencies. In *ASME Turbo Expo 2014: Turbine Technical Conference and Exposition* (pp. V01BT27A039-V01BT27A039). American Society of Mechanical Engineers.
- Tanuma, T., Y. Sasao, S. Yamamoto, Y. Niizeki, N. Shibukawa and H. Saeki (2013, June). Aerodynamic interaction effects from upstream and downstream on the down-flow type exhaust diffuser performance in a low pressure steam turbine. In *ASME Turbo Expo 2013: Turbine Technical Conference and Exposition* (pp. V05BT25A044-V05BT25A044). American Society of Mechanical Engineers.
- Tindell, R. H., T. M. Alston, C. A. Sarro, G. C. Stegmann, L. Gray and J. Davids (1996). Computational fluid dynamics analysis of a steam power plant low-pressure turbine downward exhaust hood. *Journal of engineering for gas turbines and power* 118(1), 214-224.
- Veerabathraswamy, K. and A. S. Kumar (2016). Effective boundary conditions and turbulence

S. Sadasivan *et al.* / *JAFM*, Vol. 13, No. 2, pp. 639-650, 2020.

modeling for the analysis of steam turbine exhaust hood. *Applied Thermal Engineering* 103, 773-780.

Wang, H., X. Zhu and Z. Du (2010). Aerodynamic

optimization for low pressure turbine exhaust hood using Kriging surrogate model. *International communications in heat and mass transfer* 37(8), 998-1003.